

# REV7 associates with ATRIP and inhibits ATR kinase activity

Megan Biller<sup>1,6</sup>, Sara Kabir<sup>1</sup>, Sarah Nipper<sup>1</sup>, Sydney Allen<sup>1</sup>, Yara Kayali<sup>1</sup>, Skyler Kuncik<sup>1</sup>, Hiroyuki Sasanuma<sup>2</sup>, Pei Zhou<sup>3</sup>, Cyrus Vaziri<sup>4,5</sup>, Junya Tomida<sup>1,\*</sup>

<sup>1</sup>Department of Biological Sciences, University of North Carolina at Charlotte, Charlotte, NC 28223, United States

<sup>2</sup>Department of Genome Medicine, Tokyo Metropolitan Institute of Medical Science, Tokyo 156-8506, Japan

<sup>3</sup>Department of Biochemistry, Duke University School of Medicine, Durham, NC 27710, United States

<sup>4</sup>Department of Pathology and Laboratory Medicine, University of North Carolina, Chapel Hill, NC 27599, United States

<sup>5</sup>Lineberger Comprehensive Cancer Center, University of North Carolina, Chapel Hill, NC 27599, United States

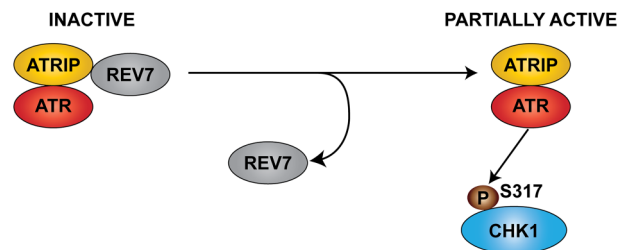
<sup>6</sup>Present address: MacroGenics Inc, Rockville, MD 20850, United States

\*To whom correspondence should be addressed. Email: [jtomida@charlotte.edu](mailto:jtomida@charlotte.edu)

## Abstract

Ataxia-telangiectasia mutated and RAD3-related (ATR) and its partner ATR-interacting protein (ATRIP) function as a critical proximal sensor and transducer of the DNA damage response (DDR). Several ATR substrates, including p53 and CHK1, are crucial for the coordination of cell cycle phase transitions, transcription, and DNA repair when cells sustain DNA damage. While much is known about ATR activation mechanisms, it is less clear how ATR signaling is negatively regulated in cells. Here, we identify the DNA repair protein REV7 as a novel direct binding partner of ATRIP. We define a REV7-interaction motif in ATRIP, which, when mutated, abrogates the REV7–ATRIP interaction *in vitro* and in intact cells. Using *in vitro* kinase assays, we show that REV7 inhibits ATR-mediated phosphorylation of its substrates, including p53. Disruption of the REV7–ATRIP interaction also enhances phosphorylation of CHK1 at Ser317 in intact cells. Taken together, our results establish REV7 as a critical negative regulator of ATR signaling. REV7 has pleiotropic roles in multiple DDR pathways, including Translesion Synthesis, DNA double-strand break resection, and p53 stability and may play a central role in the integration of multiple genome maintenance pathways.

## Graphical abstract



## Introduction

Integration of DNA replication with DNA repair, cell cycle progression, and other biological processes is crucial for preserving genome stability and is fundamentally important for all life [1, 2]. Failure to integrate these processes leads to a wide variety of developmental defects and diverse diseases ranging from dwarfism, microcephaly, progressive bone marrow failure, malignancy, and intellectual disability [3–9].

The DNA damage response (DDR) consists of multiple pathways that regulate DNA repair, DNA replication, and cell cycle progression. Key mediators of the DDR include members of the phosphoinositide 3-kinase related kinase (PIKK) family, such as ataxia-telangiectasia mutated (ATM), ataxia-

telangiectasia mutated and RAD3-related (ATR), and DNA-dependent protein kinase catalytic subunit (DNA-PKcs). These proteins are serine/threonine kinases that recognize S/TQ motifs on their substrates [10]. Members of the PIKK family contain three conserved domains: FRAP-ATM-TRRAP (FAT), FAT carboxy-terminal (FATC), and PIKK regulatory domain (PRD) [11]. FAT domains are thought to be important in cell transport. The small FATC domain is located on the C-terminus and is necessary for kinase activity. The PRD is the PIKK regulatory domain positioned between the FAT and FATC domains, which enhances kinase activity [12]. All three of these domains are thought to be important for protein–protein interactions [11].

Received: January 30, 2025. Revised: November 16, 2025. Accepted: December 3, 2025

© The Author(s) 2026. Published by Oxford University Press.

This is an Open Access article distributed under the terms of the Creative Commons Attribution-NonCommercial License

(<https://creativecommons.org/licenses/by-nc/4.0/>), which permits non-commercial re-use, distribution, and reproduction in any medium, provided the original work is properly cited. For commercial re-use, please contact [reprints@oup.com](mailto:reprints@oup.com) for reprints and translation rights for reprints. All other

permissions can be obtained through our RightsLink service via the Permissions link on the article page on our site—for further information please contact [journals.permissions@oup.com](mailto:journals.permissions@oup.com).

ATR is a critical proximal sensor and transducer of the DDR [3, 13]. While ATM and DNA-PKcs primarily respond to DNA double-strand breaks (DSBs), ATR can be activated by a wider range of genotoxic stress, including DSBs, single-stranded breaks (SSBs), and replication stress [3]. The versatility of ATR and its critical role in maintaining genome integrity during DNA replication make it indispensable for cell viability, as demonstrated by the embryonic lethality observed in *Atr* knockout mice [14].

ATR activation is a multistep process that consists of ATR recruitment to sites of damage and localization of one or more activators. The key DNA structure required for ATR activation is single-stranded DNA (ssDNA) coated by replication protein A (RPA) [15]. ssDNA is exposed after many types of DNA damage. DNA lesions encountered during replication can stall polymerases at the replication fork, resulting in stretches of exposed ssDNA. In addition, DSB end resection can result in ssDNA overhangs. To protect ssDNA from nuclease degradation, it is quickly bound by RPA [16]. RPA-ssDNA results in the localization of ATR through its obligate subunit ATRIP, which directly binds to RPA and anchors the ATR-ATRIP complex [15].

Independent of ATR localization, full activation requires the presence of an activator. Three ATR activators are currently known: TOPBP1, ETAA1, and NBS1. TOPBP1, the main activator of ATR, is directly recruited to sites of damage and requires additional factors, including the RAD17-replication factor C (RFC) complex and the RAD9-RAD1-HUS1 (9-1-1) complex. Localization of TOPBP1 recruits these complexes, and RAD17-RFC loads the 9-1-1 complex onto ss-dsDNA junctions [17]. TOPBP1 directly binds RAD9, ATR, and ATRIP, activating ATR [18]. ETAA1 acts independently of TOPBP1 and is recruited to sites of DNA damage by RPA-ssDNA, where it binds RPA through two domains. It then directly binds and activates ATR [19, 20]. NBS1 has also been shown to directly bind and activate ATR. However, unlike TOPBP1 and ETAA1, NBS1 does not contain an ATR activation domain (AAD), and the mechanisms behind its recruitment are poorly understood [21].

Once activated, ATR initiates an extensive signaling cascade, with proteomic analyses identifying over a hundred ATR substrates [22]. However, at the core of ATR signaling lie two key substrates: CHK1 and p53. Both CHK1 and p53 play significant roles in DNA repair and cell cycle progression. In response to DNA replication fork stalling, CHK1 signaling can inhibit new origin firing (the S-phase checkpoint) and slow down DNA replication, thereby integrating DNA repair with cell cycle progression [23]. CHK1 also mediates the G2 checkpoint, which ensures complete duplication of the genome before entering mitosis. p53, often referred to as the “guardian of the genome,” plays multiple roles in checkpoint signaling and DNA repair [24]. p53 is responsible for initiating the G1 checkpoint, which is critical to preventing the replication of damaged DNA [25]. The genome maintenance roles of CHK1 and p53 are critically ATR-dependent. ATR-mediated phosphorylation of CHK1 on serines 317 and 345 leads to CHK1 activation and triggers the S-phase and G2 checkpoints. ATR-dependent phosphorylation of p53 at serine 15 disrupts p53-MDM2 interactions, thereby stabilizing p53 and promoting its tumor suppressive functions [26, 27].

Attenuation of checkpoint signaling is critical for the resumption of normal cell cycle progression after DNA dam-

age is resolved. While mechanisms of ATR activation are well described, less is known regarding the negative regulation of ATR activity. Without a brake system, ATR signaling would likely persist unchecked, leading to permanent cell cycle arrest and death. It was recently reported that although ATR may be active in the absence of DNA damage, ATR-CHK1 signaling is suppressed [28]. Although a few studies have reported the mechanism of ATR downregulation [29], it remains unclear how cells prevent CHK1 signaling when ATR is active.

In our investigation of novel functions and pathways involving the DNA repair protein REV7, we identified ATRIP as a new REV7 binding partner *in vivo*. We report a novel function of the REV7-ATRIP interaction. Our findings reveal that REV7 directly interacts with ATRIP, leading to the suppression of ATR kinase activity. Through the use of a knock-in system to analyze ATRIP mutants that are incapable of binding REV7, we show that phosphorylation of CHK1 Ser317 is negatively regulated by the REV7-ATRIP interaction.

## Materials and methods

### Human cell cultures and transfections

All cells were maintained in a humidified 5% CO<sub>2</sub> incubator at 37°C. HEK293T (ATCC CRL11268) cells were cultured in Dulbecco's Modified Eagle's Medium (DMEM) (Life Technologies, Carlsbad, CA) supplemented with 10% fetal bovine serum and 1% penicillin/streptomycin (Invitrogen). Human TK6 (WT), *53BP1*<sup>-/-</sup> [30], and *REV3L*<sup>-/-</sup> [31] cell lines were obtained from Dr Hiroyuki Sasanuma, Tokyo Metropolitan Institute of Medical Science. Human TK6 cells were cultured in RPMI supplemented with 5% horse serum (Gibco™) and 1 mM sodium pyruvate (Gibco™). All cell lines were routinely assessed for mycoplasma contamination using the MycoAlert detection kit (Lonza). Cell transfection utilized a polyethyleneimine method as described previously [32–34].

### Generation of *ATRIP* knock-in TK6 cells

*ATRIP* guide RNA (gRNA) target sequence (5'-GAAAGCTTGTCTTAAGCTGGAGG-3') was inserted into the pX330 vector (Addgene, USA) for the CRISPR Cas9 system. To generate *ATRIP*<sup>P235A, P240A</sup> for TK6 cells, *ATRIP*<sup>P235A, P240A</sup> -*PUROR* and *ATRIP*<sup>P235A, P240A</sup> -*HYGR* targeting vectors, a gift from Dr Hiroyuki Sasanuma [35, 36], were produced from polymerase chain reaction (PCR)-amplified genomic products combined with *PUROR* and *HYGR* selection marker genes. PCR-amplified genomic products were amplified using the following primers: 5'-GCGAATTGGGTACCGGGCCGCTCCAGCATGGGCAACAGAGTGAGACCCTGTC-3' and 5'-CTGGGCTCGAGGGGGGCCAGTGATTCCAGTCCCTGCAGAGATTGTCCCTC-3' plus 5'-TGGGAAGCTTGTGCGACTTAAATCTATTTCAAGGTGGCTCACTCACATGGCTG-3' and 5'-CACTAGTAGGCGCGCCTTAACATTTGGGAGGCTGAAGTGGGTGGATCACG-3' for the left arm and right arm, respectively. Left and right arms were inserted into *ApaI* and *AflIII* sites of targeting vectors, respectively, using In-Fusion (Takara). All transfections in TK6 were performed as described [31, 35, 36, 37]. Cells were seeded in 96-well plates and allowed to grow. Resultant colonies were screened for *ATRIP*<sup>P235A, P240A</sup> -*PUROR* and *ATRIP*<sup>P235A, P240A</sup> -*HYGR* through integration of antibiotic resistance. After isolating

clones, *ATRIP*<sup>P235A, P240A</sup> mutations were confirmed by DNA sequencing. 1 µg pCMV-Cre (Addgene plasmid # 123 133) was transfected in  $1 \times 10^6$  *ATRIP*<sup>P235A, P240A</sup> -*PUROR* and *ATRIP*<sup>P235A, P240A</sup> -*HYGR* TK6 cells. Resultant colonies were screened for *ATRIP*<sup>P235A, P240A</sup> through the confirmation of antibiotic sensitivity.

### DNA damage treatment

TK6 (WT, *REV7*<sup>-/-</sup>, *REV3L*<sup>-/-</sup>, and *53BP1*<sup>-/-</sup>) cell lines were seeded in T25 flasks at a concentration of  $2 \times 10^5$  cells/mL. Cells were treated with 40 ng/ml mitomycin C (MMC), 40 µM hydroxyurea (HU), or control. 24 h later,  $4 \times 10^6$  cells were harvested and resuspended in 200 µl of 1× SDS loading buffer as described previously [34]. Samples were sonicated (30% amplitude, four cycles of 15 s with a 30-s pause). 42 h after transfection, 293T cells were treated with 2 mM HU or mock for 6 h. Cells were then harvested, resuspended in 200 µl of 1× SDS loading buffer, and sonicated (30% amplitude, four cycles of 15 s with a 30-s pause). For the time course experiment, TK6 cells were treated with 40 µM hydroxyurea (HU) or were left untreated for controls. 2, 4, 8, and 16 h later,  $4 \times 10^6$  cells were harvested and resuspended in 200 µl of 1× SDS loading buffer as described previously [34].

### Protein purification, GST pulldown, immunoprecipitation, and immunoblotting

Proteins were purified from *Escherichia coli* as described previously [34, 38–40]. His-REV7 and GST purification were performed as described [34]. Immunoprecipitation and immunoblotting were described previously [41–43]. The samples were separated by polyacrylamide gel electrophoresis, transferred to a membrane, and detected with the indicated antibodies and ECL reagents (GE Healthcare) or IRDye 800 (Li-Cor).

### ATR kinase assays

Kinase assays were performed as described previously [34].

### Antibodies

Antibodies purchased along with dilutions used for immunoblotting were as follows:

The polyclonal anti-REV7/MAD2L2 (12683-1-AP), WB 1:1 200, IP 1:200, was purchased from ProteinTech. Anti-ATRIP (A300-670A), 1:1 000, was obtained from Thermo Fisher Scientific. P-p53 Ser15 (9284), 1:1 000; P-ATR Thr1989 (30 632), 1:1 000; P-Chk1 Ser345 (2348), 1:1 000; monoclonal anti-HA (3724), 1:1 000; and P-Chk1 Ser317 (12 302), 1:1 000, were obtained from Cell Signaling. MAD2B (612 266), 1:1 200, was purchased from BD Biosciences. A2220, anti-FLAG M2 affinity agarose gel; F3165, monoclonal anti-FLAG 1:10 000; T5168, monoclonal anti-α-Tubulin 1:8 000; A0168 HRP (horseradish peroxidase) conjugated anti-mouse IgG 1:10 000; and A0545 HRP conjugated anti-rabbit IgG 1:10 000 were purchased from Sigma-Aldrich. IRDye 800 CW Goat anti-Mouse IgG Secondary Antibody (926–32 210), 1:20 000, and IRDye 800 CW Goat anti-Rabbit IgG Secondary Antibody (926–32 211), 1:20 000, were purchased from Li-Cor. Anti-GST (SC-138), 1:400; p53 (sc-126), 1:200; CHK1 (sc-8408), 1:2 500; and ATR (sc-515173) 1:200, were purchased from Santa Cruz Biotechnology. Anti-

V5 (ab27671), WB 1:1 000, IP 1:300, was obtained from Abcam Inc.

### DNA constructs

The human His-REV7 (pEtDuet-1-REV7) [40], pCDH-EF1α-MCS-Flag-HA-IRES-Puro [44], pCDH-EF1a-V5-REV7-IRES-Puro [45], and the following shRNA vector shREV7#2 (TRCN000006569) were gifted from Dr. Richard Wood. shScramble shRNA was obtained from Dr. David Sabatini (Addgene plasmid # 1864) [46]. The Flag-ATR expression vectors were a gift from Dr. Karlene A. Cimprich [47]. The human *ATRIP* wild type (WT) full-length cDNA was obtained from Dr. Minoru Takata [41]. After construction, expression vectors were confirmed by DNA sequencing. p53: GST-p53 2–50 fragment expression vector was described previously [34]. ATRIP: GST-ATRIP fragments were purified as an XhoI–NotI fragment from the ATRIP expression vector and cloned into pGEX6P-1 (GE Healthcare). GST-ATRIP 1–107, 1–348, 108–348, 203–348, 203–791, 203–307, 349–507, 508–791 fragments were PCR amplified from ATRIP-GFP expression vector as XhoI–NotI fragments with 5′ATRIP (XhoI) primer (5′-CCGCTCGAGATGGCGGGGACCTCCGCGCCAGGC) and 3′ ATRIP 107 (NotI) primer (5′-TAAAAGCGGC CGCTCATGGAACAGTTTCTCTGTTTTTC), 5′ATRIP (XhoI) primer (5′-CCGCTCGAGATGGCGGGGACCT CCGCGCCAGGC) and 3′ ATRIP 348 (NotI) primer (5′-TAAAAGCGGCCGCTCATGGTGGCTGCAGGGGGGT GCCAG), 5′ATRIP 108 (XhoI) primer (5′-CCGCTCGAGA TAAAAGATAATTTTCGAATTAGAG) and 3′ ATRIP 348 (NotI) primer (5′-TAAAAGCGGCCGCTCATGGTGGCT GCAGGGGGTGCCAG), 5′ATRIP 203 (XhoI) primer (5′-CCGCTCGAGAGGACAAAGCTCCAGACCAGTGAAC) and 3′ ATRIP 348 (NotI) primer (5′-TAAAAGCG GCCGCTCATGGTGGCTGCAGGGGGGTGCCAG), 5′ATRIP 203 (XhoI) primer (5′-CCGCTCGAGAGGAC AAAGCTCCAGACCAGTGAAC) and 3′ ATRIP (NotI) primer (5′-TAAAAGCGGCCGCTCAGCCACACTCCAC CTCGGGGTCTTC), 5′ATRIP 203 (XhoI) primer (5′-CCGCTCGAGAGGACAAAGCTCCAGACCAGTGAAC) and 3′ ATRIP-307 rev (NotI) primer (5′-CAGTCAGTCAG ATCGGGCTCAAGTGTGTTGATCTCTGTCTCCAGCTG), 5′ATRIP 349 (XhoI) primer (5′-CCGCTCGAGGGGTT TGGCAGTACCTTGGCTGGAATG) and 3′ ATRIP 507 (NotI) primer (5′-TAAAAGCGGCCGCTCACCCAGCAG CAGAATCTGCCCC), and 5′ATRIP 508 (XhoI) primer (5′-CCGCTCGAGGAAGGAAACAGGAGCCTGGTTCAC) and 3′ ATRIP (NotI) primer (5′-TAAAAGCGGCCGCTCAGCCA CACTCCACCTCGGGGTCTTC) to clone into pGEX6P-1 (GE Healthcare). ATRIP (P235A, P240A) mutations were introduced using site-directed mutagenesis (TOYOBO KOD FX). The XhoI–NotI fragments from WT *ATRIP* or *ATRIP* (P235A and P240A) were inserted into pCDH-EF1α-Flag-HA-MCS-IRES-Puro to generate FH-ATRIP, ATRIP-FH, and ATRIP (P235A and P240A)-FH (P235A and P240A).

### Quantification

Histograms from western blots (Supplemental Raw Data Figs 6, 7, and 8) were created using ImageJ software. Signal intensity was calculated by ImageJ software, with the average signal intensity ( $n = 3$ ) used for the calculations in Figs 3A, 4A, B, 5A, and D, and in Supplemental Figs 3, 4A, 5, and 7. The signals of phosphorylated CHK1 Ser317 and Ser345 were nor-

malized to CHK1. The signals of ATR and ATRIP in Fig. 5A were normalized to  $\alpha$ Tubulin. The signals of ATR and ATRIP in Fig. 5D were normalized to REV7. The signal of ATR in Supplemental Fig. 3 was normalized to Flag. The signals of phosphorylated ATR in Supplemental Fig. 5 were normalized to  $\alpha$ Tubulin. The signals of p53, phosphorylated p53 Ser15, REV7, ATR, and ATRIP in Supplemental Fig. 7 were normalized to  $\alpha$ Tubulin.

### Mass spectrometric analysis of purified REV7 complexes

Purification of the REV7 complex and analysis by LC-MS/MS has been described [43].

### FACS analysis

Cells were pulse-labeled with BrdU (10  $\mu$ M, 1h) and analyzed by FACS as described [48–50].

### Molecular modeling

The sequences of human REV7 (UniProt: Q9UI95) and a peptide of ATRIP (residues 232–242: VIKPEACSPQF) were used as the input for the ColabFold [51] implementation of AlphaFold-Multimer (<https://www.biorxiv.org/content/10.1101/2021.10.04.463034v2>) to build the AlphaFold2 model [52] of the REV7–ATRIP peptide complex, with an excellent convergence for all five models.

## Results and discussion

### REV7 directly interacts with ATRIP

In a previous study, we performed mass spectrometry analysis of REV7 complexes from mammalian cells and identified FAM35A as a REV7-interacting protein [43]. In the same mass spectrometry dataset, we also identified endogenous ATR and ATRIP as components of the REV7 complex (Fig. 1A). To verify that ATRIP indeed associates with REV7, we ectopically expressed C-terminally FLAG-HA-tagged ATRIP (ATRIP-FH) or N-terminally FLAG-HA-tagged-ATRIP (FH-ATRIP) in 293T cells. We then immunoprecipitated the two epitope-tagged ATRIP variants using FLAG antibodies and analyzed those complexes using SDS-PAGE and immunoblotting with anti-REV7 antibodies. As shown in Fig. 1B, FH-ATRIP and ATRIP-FH both specifically co-immunoprecipitated with endogenous REV7, showing that ATRIP and REV7 exist in the same protein complex in human cells (Fig. 1B). This result was confirmed by co-immunoprecipitation using anti-REV7, which showed that endogenous REV7 complexes pulled down endogenous ATRIP, but not with beads alone (Fig. 1C).

Previous work identified a REV7-binding site  $\phi\phi$ PxxxxP (where  $\phi$  represents an aliphatic amino acid residue) [40, 53] at residues 1877–1887 and 1993–2003 of the REV7-binding partner REV3L (Fig. 1D). Interestingly, our sequence analyses revealed this consensus REV7-binding sequence motif at residues 232–240 in human ATRIP, but not in human ATR (Fig. 1D). The REV7-binding sequence in human ATRIP is conserved in *Pan troglodytes* (Chimpanzee), *Macaca mulatta* (monkey), *Canis lupus familiaris* (dog), and *Bos taurus* (cattle), but not in Rodentia species, including *Mus musculus* and *Rattus norvegicus* (Supplementary Fig. S2), indicative of a conserved role for the ATRIP-REV7 complex in higher mammals.

To test whether the region of ATRIP 204–348 can bind to REV7, we purified full-length His-REV7 and several GST fusion fragments of ATRIP in *E. coli* (Fig. 1E). We then measured *in vitro* binding of GST-tagged ATRIP fragments with recombinant His-REV7. Our GST pull-down experiments revealed that His-REV7 associated only with GST-ATRIP fragments containing amino acids P235 and P240 (Fig. 1F). We conclude that REV7 interacts directly with a 145-amino acid region of ATRIP containing a consensus REV7-interaction motif.

### REV7 interacts with ATRIP at P235 and P240

Next, we asked whether the conserved prolines (P235 and P240) in ATRIP function as REV7 binding sites. Therefore, we expressed GST-tagged ATRIP fragments spanning residues 203–307 in which these proline residues were conditionally mutated to alanine (P235A and P240A) (Fig. 2A). In GST pull-down assays, His-REV7 bound readily to GST-ATRIP 203–307 (WT), but not to GST-ATRIP 203–307 (P235A and P240A) (Fig. 2B), confirming that P235 and P240 mediate the REV7–ATRIP interaction.

We considered the potential for additional REV7 binding sites in the ATR–ATRIP complex. To test this possibility, 293T cells were transfected with full-length ATRIP-FH or with REV7 binding mutants (P235A and P240A). The ATRIP mutant with consensus REV7-binding site substitutions (P235A and P240A) completely failed to co-immunoprecipitate endogenous REV7, but its association with endogenous ATR was intact (Figs 2C and Supplementary Fig. S3). This result was verified by reciprocal co-immunoprecipitation experiments in which wild-type V5-REV7 complexes pulled down wild-type ATRIP-FH but not the ATRIP-FH mutant containing P235A and P240A substitutions in the REV7 binding domain (Fig. 2D).

Therefore, REV7 interacts directly with residues P235 and P240 of the ATRIP protein. Interestingly, a previous study established the TOPBP1 binding domain of ATRIP (204 - 308) [54], which includes the REV7 binding sites (P235 and P240). This suggests that ATRIP binds to multiple DDR partners via a common domain.

### REV7 inhibits ATR kinase activity

Next, we asked whether the REV7–ATRIP interaction influences ATR protein kinase activity. We performed *in vitro* ATR kinase assays using a recombinant GST-p53 protein (containing residues 2–50, which includes the ATR target site Ser15) as a biologically relevant ATR kinase substrate. Since this p53 fragment does not interact with REV7 [34], the possibility of a REV7-substrate interaction affecting the results is excluded.

As expected, immunoprecipitated FLAG-ATR from 293T cells readily phosphorylated GST-p53 (Fig. 3A). Interestingly, FLAG-ATR-dependent phosphorylation of p53 Ser15 decreased drastically ( $\sim$ 97%) with the addition of purified His-REV7 (Fig. 3A), suggesting that the REV7–ATRIP interaction inhibits the ability of the ATR complex to phosphorylate its substrates.

To test the hypothesis that REV7 is a biologically relevant negative regulator of ATR signaling, we examined the impact of REV7 loss on the DDR in intact cells. We used gene editing to generate isogenic WT and REV7<sup>-/-</sup> (designated “REV7 KO”) TK6 cells. Using these cells, we measured phosphorylation of CHK1 Ser317, CHK1 Ser345, and p53 Ser15 as a direct readout of ATR activity following conditional treatment

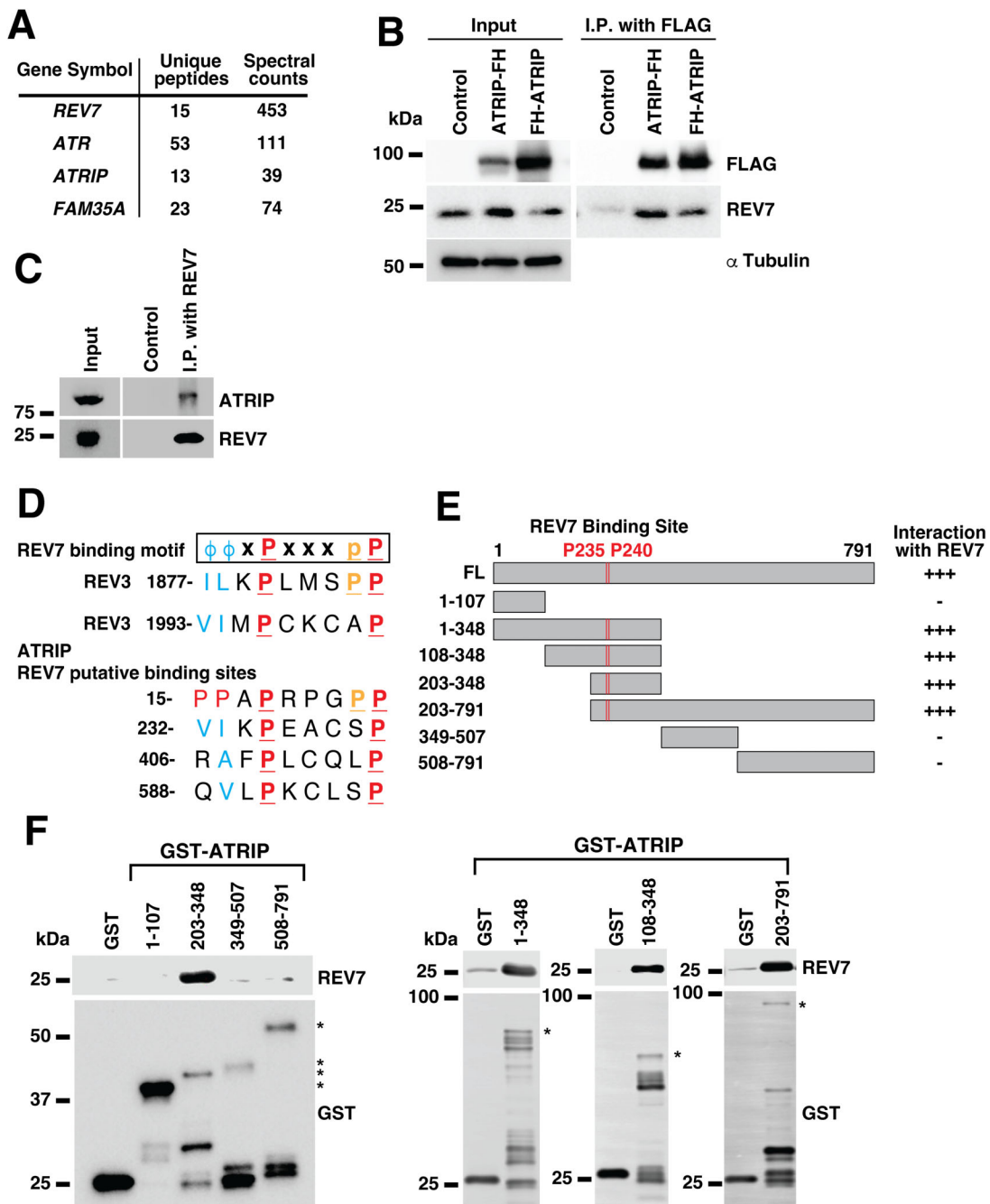


**Figure 1.** REV7 interacts with the ATR–ATRIP complex. **(A)** REV7 mass spectrometry analysis. The REV7–FH complex was sequentially immunoprecipitated (using FLAG and HA antibody beads) from nuclear extracts of HeLa S3 cell lines stably expressing C-terminally FLAG-HA-tagged REV7 (REV7–FH). A partial list of REV7–FH-associated proteins was identified in the mass spectrometry analysis previously carried out by Tomida *et al.* The results from the mass spectrometry analysis are shown in the table. A number of unique peptides and spectral counts (the number of total peptides) were described. **(B)** Co-immunoprecipitation of ATRIP–FH or FH–ATRIP and endogenous REV7 from 293T cells. C-terminally FLAG-HA-tagged ATRIP (ATRIP-FH), (N-terminally FLAG-HA-tagged-ATRIP (FH–ATRIP), or empty vector (control) were transfected into human 293T cells. Thirty hours after transfection, cell lysates were made and used for immunoprecipitation with FLAG antibody beads. After the electrophoretic transfer of proteins, the membrane was immunoblotted with the indicated antibodies. After gel electrophoresis, results for the input and immunoprecipitation (IP) product are shown. See also [Supplemental Raw Data Fig. 1](#). **(C)** Co-immunoprecipitation of both endogenous REV7 and ATRIP from 293T cells. Cell lysates were made and used for immunoprecipitation with REV7 antibody and beads. After the electrophoretic transfer of proteins, the membrane was immunoblotted with the indicated antibodies. After gel electrophoresis, results for the input and immunoprecipitation (IP) product are shown. See also [Supplemental Raw Data Fig. 1](#). **(D)** Sequence alignments of a region of REV3L, showing the REV7 binding sites, and ATRIP with the consensus sequence  $\phi \phi x P x x x P P$  at the top. Numbers refer to human ATRIP residues.  $\phi$  is an aliphatic amino acid,  $x$  is any amino acid,  $P$  is a highly conserved proline, and  $p$  is a less-conserved proline. **(E)** Schematic showing locations of the ATRIP fragments GST-ATRIP amino-acid residues, 1–107, 1–348, 108–348, 203–348, 203–791, 349–507, and 508–791. The P235/P240 position is indicated by a vertical bar. See also [Supplemental Raw Data Fig. 1](#). **(F)** *In vitro* association of REV7 with fragments of ATRIP. GST fusion fragments of ATRIP and His-REV7 fusion protein were purified from *E. coli* (see [Supplementary Fig. S1](#)). Asterisks (\*) indicate the predicted molecular weights of GST fusion fragments of ATRIP. These were used with glutathione beads for GST pull-down experiments. After electrophoresis, samples were immunoblotted with anti-REV7 or anti-GST as indicated. See also [Supplemental Raw Data Fig. 1](#).

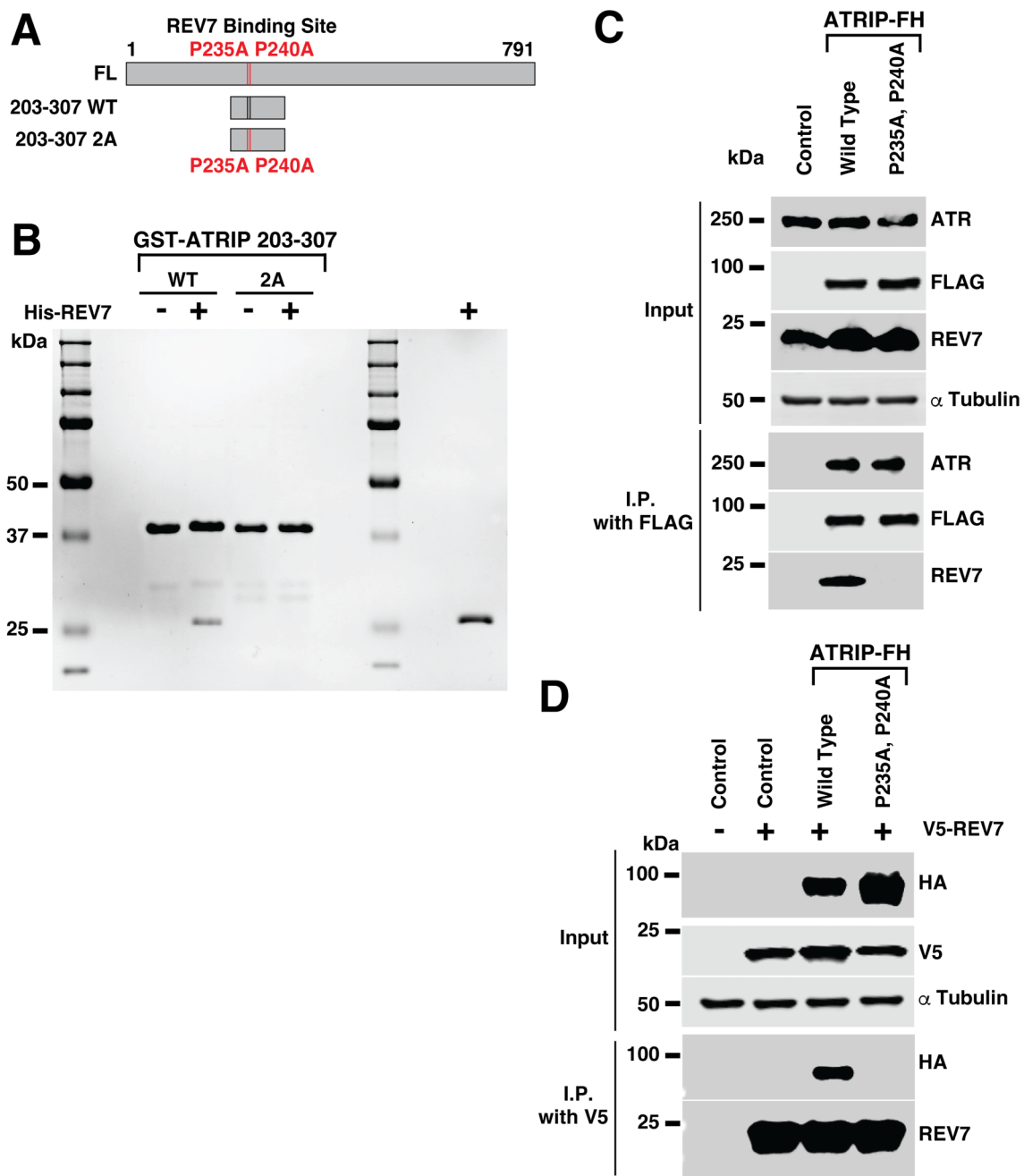


**Figure 2.** REV7 directly interacts with ATRIP at P235 and P240. **(A)** Schematic drawing showing locations of the ATRIP fragments. The P235/P240 position is highlighted with a vertical bar. **(B)** *In vitro* GST pull-down of purified ATRIP fragments (see [Supplementary Fig. S1](#)) containing the indicated amino acid changes. After electrophoresis, samples were stained with Coomassie brilliant blue. **(C)** FLAG-IP assay of 293T cells transfected with ATRIP-FH, ATRIP-FH (P235A and P240A), or control empty vector. Cells were harvested 48 h after transfection, and immunoprecipitation (IP) was performed using M2 agarose beads. For immunoblotting, we used anti-FLAG, anti-ATR, anti-REV7, and anti- $\alpha$ Tubulin. See also [Supplemental Raw Data Fig. 2](#). **(D)** V5-IP assay of 293T cells co-transfected with V5-REV7 and ATRIP-FH, ATRIP-FH (P235A and P240A), or control empty vector. Cells were harvested 48 h after transfection, and IP was performed using V5 antibody and A/G agarose. For immunoblotting, we used anti-HA, anti-V5 (as REV7), anti-REV7, and anti- $\alpha$ Tubulin. See also [Supplemental Raw Data Fig. 2](#).

with 24-h mitomycin (MMC) or hydroxyurea (HU). Separately, we measured ATR activity at 0, 2, 4, 8, and 16-h time-points during an exposure to HU (or mock treatment for control) in WT and *REV7* KO cells. The signal intensity of HU-induced CHK1 Ser317 phosphorylation was similar among WT and *REV7* KO cell lines, which express only endogenous ATR and ATRIP (1:1.1:1.4) ([Supplementary Fig. S4A](#)). In WT cells, p53 Ser15 phosphorylation increased after 16 h

of HU treatment ([Supplementary Fig. S4B](#)). In *REV7* KO cells, the signal of p53 and phosphorylation of p53 Ser15 was substantially higher than in WT. These data are consistent with our previous report [34] showing that REV7 is a negative regulator of ATM-mediated p53 phosphorylation. Surprisingly, in *REV7* KO cells, CHK1 Ser317 phosphorylation increased without DNA damage-inducing agents (Figs 3B and [Supplementary Fig. S4B](#)), a signal that was rescued by

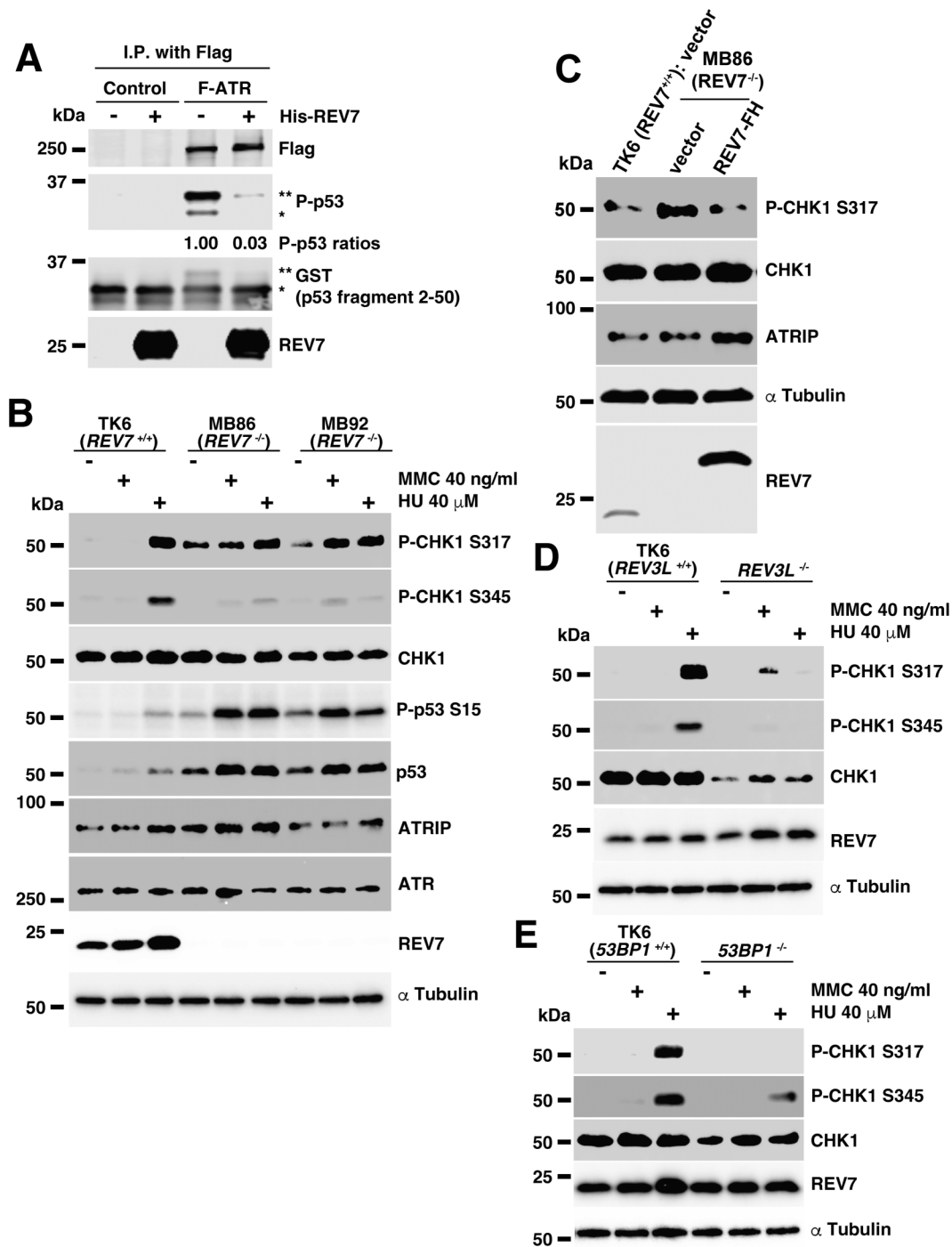


**Figure 3.** REV7 inhibits ATR activity. **(A)** REV7 disassociated p53 fragment (2–50) affects ATR kinase activity *in vitro*. 293T cells were transfected with Flag-tagged ATR (F-ATR) or empty vector control. Cells were harvested 48 h after transfection, and immunoprecipitation was performed using M2 agarose beads. The beads were washed twice with kinase buffer. 10 μl of buffer or 10 μg of His-REV7 were added, and samples were incubated at 30°C for 15 min. 10 μl of reaction buffer containing substrate (purified GST-p53 fragment) was added, followed by a 30 min incubation at 30°C. After electrophoretic transfer of proteins, the membrane was immunoblotted with the indicated antibodies. Results for the immunoprecipitation (IP) product after gel electrophoresis are shown. The shifted P-p53 Ser15 bands (\*\*\*) and (\*) are the same size as the shifted GST-p53 (2–50) (\*\*\*) and GST-p53 (2–50) (\*) bands, respectively. **(B)** western blot of DDR activation following a 24-h 40 ng/ml mitomycin C (MMC), 40 μM hydroxyurea (HU), or mock exposure in TK6 (REV7<sup>+/+</sup>), MB86 (REV7<sup>-/-</sup>), and MB92 (REV7<sup>-/-</sup>) cells. Protein loading was equalized based on cell number. After the electrophoretic transfer of proteins, the western blot membranes were immunoblotted with the appropriate antibodies. **(C)** The increase in phospho-CHK1 (Ser317) (P-CHK1 S317) protein was rescued when we complemented REV7<sup>-/-</sup> cells with a REV7 expression vector. Protein loading was equalized based on cell number. Expression of CHK1, phospho-CHK1 (Ser317), phospho-CHK1 (Ser345) (P-CHK1 S345), phospho-p53 (Ser15) (P-p53 S15), p53, αTubulin, REV7, ATR, and ATRIP proteins was determined by western blot in TK6 (REV7<sup>+/+</sup>) with empty vector and MB86 (REV7<sup>-/-</sup>) cells with empty vector or REV7-FH. **(D-E)** western blot of DDR activation following a 24-h 40 ng/ml mitomycin C (MMC), 40 μM hydroxyurea (HU), or mock exposure in TK6, REV3L<sup>-/-</sup> **(D)** or 53BP1<sup>-/-</sup> **(E)** TK6 cells. Protein loading was equalized based on cell number. After the electrophoretic transfer of proteins, the western blot membranes were immunoblotted with the appropriate antibodies. See also [Supplemental Raw Data Figs 3 and 6](#).

stable re-expression of REV7-FH (Fig. 3C). Previous studies have demonstrated that CHK1 phosphorylation at S317 precedes and is required for subsequent CHK1 S345 phosphorylation, which fully activates CHK1. However, the mechanisms governing the progression from p-CHK1 S317 to p-CHK1 S345 are unclear. Studies using phospho-mimetic mutations CHK1 S317E or S317D have shown that p-CHK1 S317 alone is insufficient to induce p-CHK1 S345; however, the accuracy of these mutations in modeling p-CHK1 S317 is uncertain [55–57]. Notably, p-CHK1 S317 without concurrent p-CHK1 S345 has not been reported in cellular studies. Therefore, we propose that a novel mechanism of p-CHK1 S317 induction is a critical step in the transition of CHK1 to its fully activated state. Altogether, our findings suggest that REV7 specifically regulates CHK1 Ser317 phosphorylation.

The results of Fig. 3 are consistent with our finding that REV7 inhibits ATR, and that *REV7* deletion leads to de-repression of ATR kinase activity towards its key substrates CHK1 and p53. We note that REV7 associates with REV3L to form the TLS extender polymerase Pol $\zeta$ , and TLS deficiency has previously been shown to lead to persistent replication stalling and compensatory increases in ATR-CHK signaling [58, 59]. Therefore, we performed additional experiments to determine whether the increased CHK1 Ser317 phosphorylation in *REV7* KO cells could be explained by decreases in Pol $\zeta$ -mediated TLS activity. As an experimental strategy for inhibiting Pol $\zeta$ -mediated TLS independently of *REV7* deletion, we tested *REV3L*<sup>-/-</sup> cells. As shown in Fig. 3D, *REV3L* KO cells did not show increases in CHK1 Serine 317 or Serine 345 phosphorylation, showing that the increased CHK1 phosphorylation in *REV7* KO cells cannot be attributed to lack of Pol $\zeta$ .

In addition to its role as a subunit of Pol $\zeta$ , REV7 is a component of the Shieldin antiresection complex. Therefore, we also considered the formal possibility that the stimulatory effects of *REV7* loss on CHK1 phosphorylation were related to DSB resection. To inhibit DSB anti-resection without depleting REV7, we generated cells lacking 53BP1. As shown in Fig. 3E, deletion of *53BP1* had no effect on CHK1 Serine 317 or Serine 345 phosphorylation without DNA damage induction. Therefore, we conclude that the stimulatory effect of *REV7* loss on CHK1 Ser317 phosphorylation cannot be attributed to increased DSB resection.

### Phosphorylation of CHK1 Ser317 is regulated by REV7–ATRIP binding in intact cells

Next, we sought to verify that the ATR–CHK1 signaling axis is regulated by REV7–ATRIP interactions in intact cells. We co-transfected 293T cells with vectors encoding ATR and WT or REV7-interaction-deficient (P235A and P240A) ATRIP. The ATR/ATRIP-co-expressing cells (and empty vector controls) were conditionally treated with HU to induce S-phase checkpoint signaling. Then we determined the effects of these treatments on levels of CHK1 Ser317, CHK1 Ser345, and ATR Thr1989 phosphorylation as a measure of ATR activity.

Strikingly, transient co-expression of F-ATR with REV7-interaction-defective ATRIP led to higher levels of CHK1 Ser317 phosphorylation (~twofold) when compared with cells co-expressing F-ATR with ATRIP (WT), whereas levels of CHK1 Ser345 phosphorylation were unchanged (Fig. 4A). ATR Thr1989 phosphorylation was similar among control cells (no expression of F-ATR and ATRIP-FH), co-

expressing F-ATR with ATRIP (WT), and co-expressing F-ATR with ATRIP (P235A, P240A) (1:1.1:1) (Supplementary Fig. S5). These data show that overexpression of F-ATR and ATRIP-FH inhibits CHK1 phosphorylation (Supplementary Fig. S5). This inhibition occurs because the overexpressed ATR–ATRIP exceeds endogenous REV7. However, REV7-interaction-deficient ATRIP restores CHK1 Ser317 phosphorylation.

We also determined the effect of REV7-depletion on CHK1 Ser317 phosphorylation in cells expressing WT or REV7-interaction-deficient forms of ATRIP. As expected, REV7 depletion led to increases in HU-induced CHK1 Ser317 phosphorylation in cells expressing WT ATRIP (~threefold) (Fig. 4B). In contrast, in cells expressing ATRIP (P235A, P240A), CHK1 Ser317 phosphorylation was relatively insensitive to REV7 depletion (~1.3-fold) (Fig. 4B). Taken together, the results of Fig. 4 demonstrate that in intact cells, REV7 represses CHK1 Ser317 phosphorylation by ATR, in a manner that depends on the REV7–ATRIP interaction. Importantly, the *in vivo* repression of ATR signaling by the REV7–ATRIP interaction fully recapitulates our biochemical studies with isolated proteins.

### CHK1 Ser317 phosphorylation accumulates in cells expressing REV7 binding mutant ATRIP without DNA damage induction

To further define the effect of the REV7–ATRIP interaction on ATR–CHK1 signaling, and to complement our ATR–ATRIP overexpression studies in 293T cells (Fig. 4), we used a knock-in approach to alter endogenous *ATRIP* alleles in diploid TK6 cell lines. Supplementary Fig. S6 describes the gene targeting strategy we used to generate TK6 cells harboring proline (P) to alanine (A) codon substitutions in the endogenous *ATRIP* alleles.

To determine how the REV7–ATRIP interaction affects ATR–CHK1 signaling in TK6 cells, we compared phosphorylation of ATR substrates (CHK1 Ser317, CHK1 Ser345, and p53 Ser15) in two independent clones of *ATRIP*<sup>P235A, P240A</sup> TK6 cells and in an isogenic parental cell line. We determined phosphorylation of ATR substrates in all three cell lines both basally and after treatment with HU.

As expected based on our *in vitro* experiments with 293T cells, *ATRIP*<sup>P235A, P240A</sup> increased CHK1 Ser317 phosphorylation without DNA damage-inducing agents (~12-fold). After HU treatment, CHK1 Ser317 phosphorylation further increased in *ATRIP*<sup>P235A, P240A</sup> (Fig. 5A). This result suggests that ablation of REV7–ATRIP binding does not affect the TOPBP1–ATRIP interaction, which is necessary for full activation of ATR. Interestingly, despite the reduced expression of ATR and ATRIP proteins in cells expressing the ATRIP mutants (70% and 50%, respectively, when compared with WT), the P-CHK1 Ser317 signal in ATRIP mutants was higher (1.8 and 1.4-fold each) than in WT following HU treatment (Fig. 5A). The P-CHK1 Ser345 signal was similarly elevated in ATRIP mutants following DNA damage (1.7 and 1.4-fold each). Similar to *REV7* KO cells (Fig. 3B), *ATRIP*<sup>P235A, P240A</sup> cells did not show elevated p53 or P-p53 Ser15 when compared with WT (Figs 5A and Supplementary Fig. S7). Our previous report revealed a marked decrease in the S-phase population of *REV7* KO cells relative to WT [34]. Therefore, to test whether REV7-interaction-defective ATRIP causes cell cycle arrest, we examined cell cycle profiles of WT

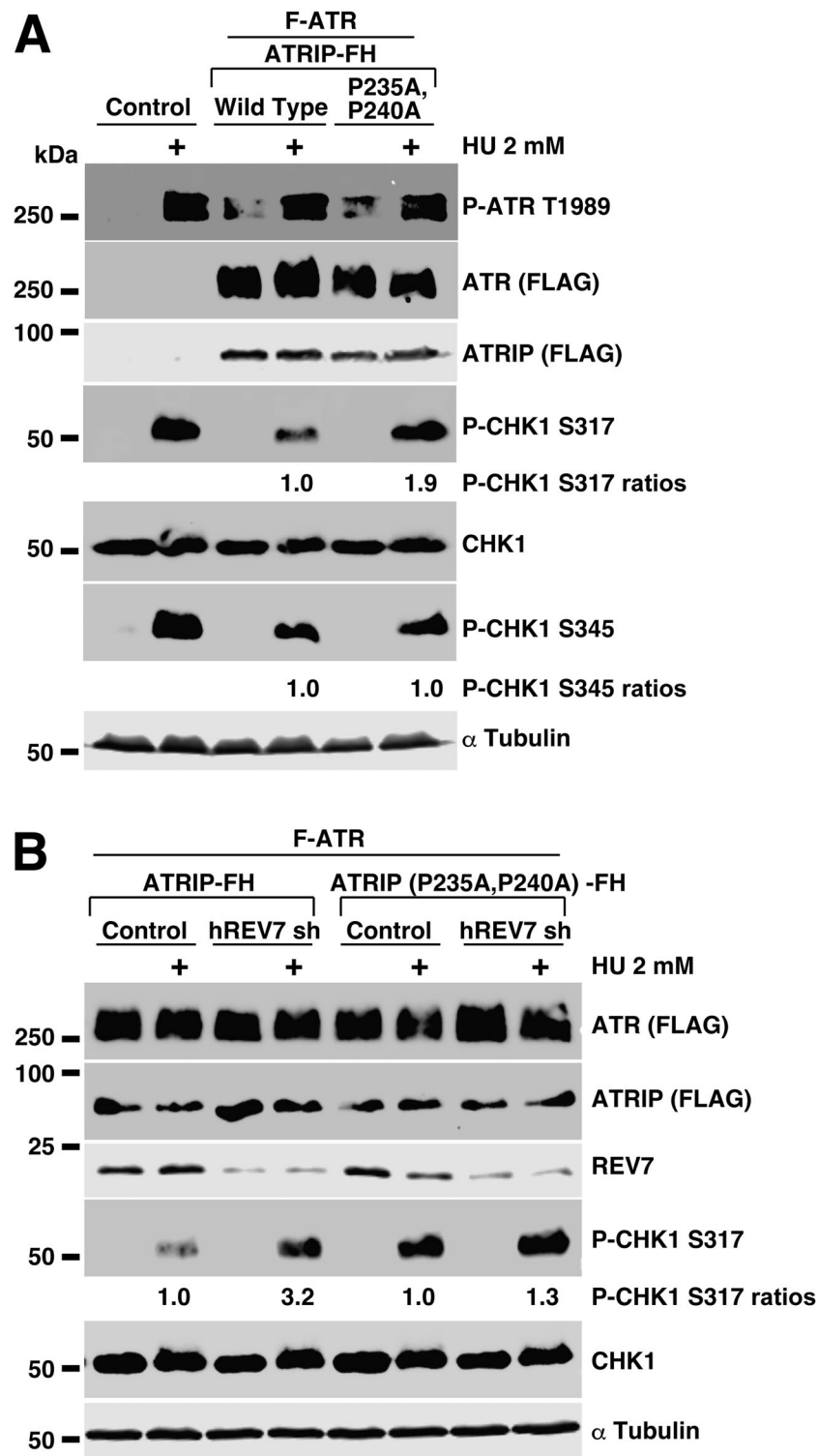


**Figure 4.** REV7 inhibits Ser317 phosphorylation of CHK1 via ATRIP binding. **(A)** REV7-disassociated ATRIP increases Ser317 phosphorylation of CHK1. FLAG-tagged ATR (F-ATR) was co-transfected into human 293T cells with empty vector (Control), ATRIP-FH, or ATRIP-FH (P235A, P240A). 42 h after transfection, cells were treated for 6 h with 2 mM hydroxyurea (HU) or mock. Cells were then harvested and used for western blot. After the electrophoretic transfer of proteins, the western blot membranes were immunoblotted with the appropriate antibodies. **(B)** REV7 depletion increases Ser317 phosphorylation of CHK1 in ATR-ATRIP expressing cells but not in cells expressing REV7-disassociated ATRIP. FLAG-tagged ATR (F-ATR) was co-transfected into human 293T cells with ATRIP-FH and shRNA Scramble (Control) or shRNA REV7 (hREV7 sh) and ATRIP-FH (P235A, P240A) and shRNA Scramble (Control) or shRNA REV7 (hREV7 sh). 42 h after transfection, cells were treated for 6 h with 2 mM hydroxyurea (HU) or mock. Cells were harvested and used for western blot. After the electrophoretic transfer of proteins, the western blot membranes were immunoblotted with the appropriate antibodies. See also [Supplemental Raw Data Figs 4 and 6](#).

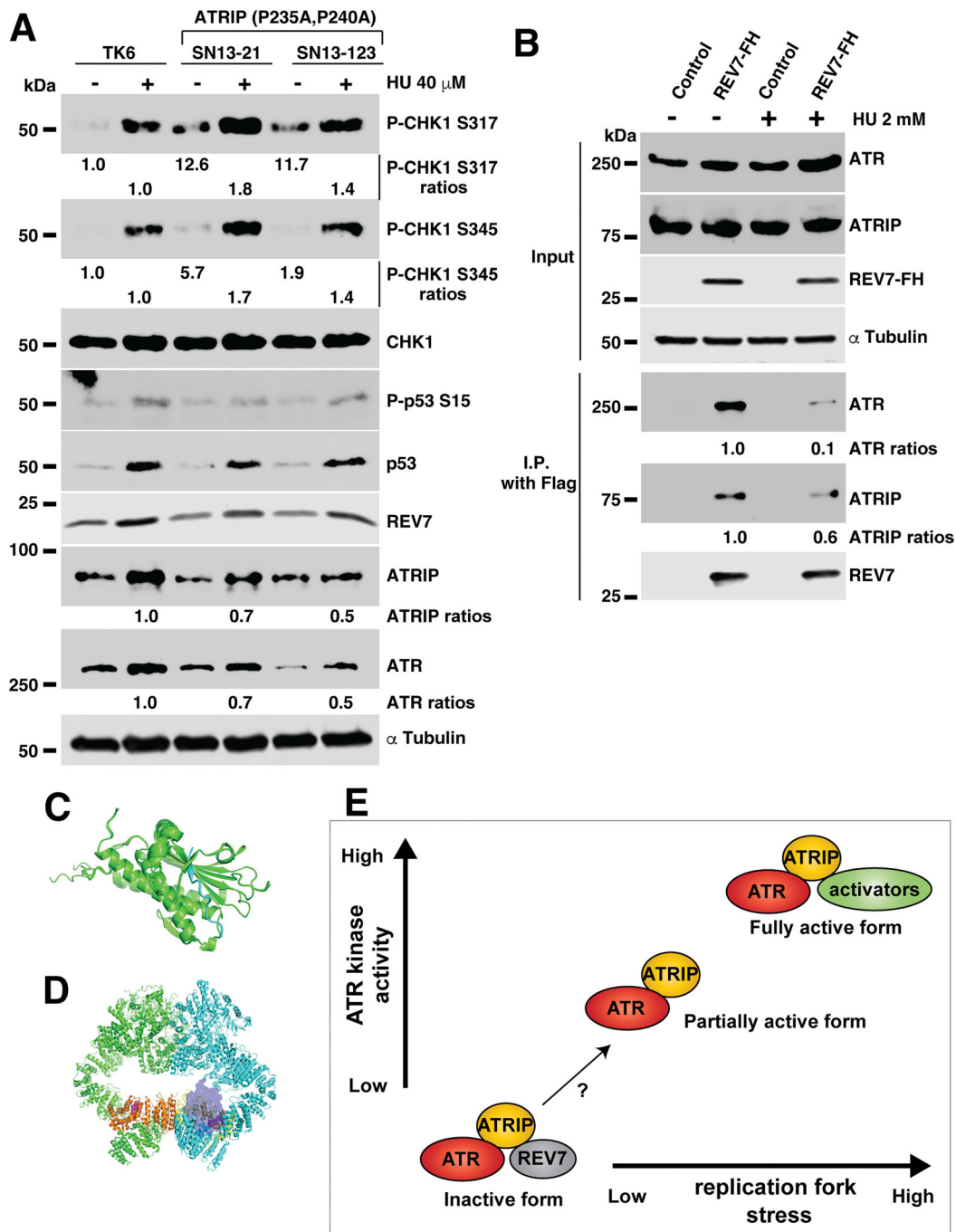


**Figure 5.** REV7-ATRIP-ATR is the inactive form of the ATR complex. **(A)** Western blot of DDR activation. CHK1 phosphorylation of Serine 317 was examined following a 24-h exposure to 40  $\mu$ M hydroxyurea (HU) exposure in TK6, SN13-21 (ATRIPP235A, P240A/P235A, P240A), and SN13-123 (ATRIPP235A, P240A/P235A, and P240A) cells. Protein loading was equalized based on cell number. After the electrophoretic transfer of proteins, the western blot membranes were immunoblotted with the appropriate antibodies. See also [Supplemental Raw Data Figs 5 and 7](#). **(B)** Levels of ATR and ATRIP proteins decreased in the REV7 immunoprecipitation (IP) product following a 6-h, 2 mM hydroxyurea (HU) exposure. FLAG-HA-tagged REV7 was transfected into human 293T cells. 42 h after transfection, cells were treated for 6 h with 2 mM hydroxyurea (HU) or mock. Cells were harvested, and IP was performed using M2 agarose beads. After the electrophoretic transfer of proteins, the western blot membranes were immunoblotted with the appropriate antibodies. See also [Supplemental Raw Data Figs 5 and 7](#). **(C)** AlphaFold model of the ATRIP-REV7 complex from ColabFold implementation of the AlphaFold-multimer. Green indicates REV7. Blue indicates REV7 binding site peptide "VIKPEACSPQF" in ATRIP. **(D)** ATR-ATRIP complex with overlay of the REV7 binding site peptide. Green/cyan indicates ATR. Orange/yellow indicates ATRIP. The ATRIP peptide "VIKPEACSPQF" is purple (in space filling). **(E)** Model of functional interactions between REV7 and ATRIP. Bottom left: The REV7-ATRIP-ATR complex is the inactive form. REV7 interacts with ATRIP via P235 and P240 within the  $\phi\phi$ PxxxP motif, which is known to bind to the safety belt region of REV7. By binding to ATRIP, REV7 may induce a conformational change in the ATR complex that prevents CHK1 signaling. Functionally, this interaction could be significant, as it may enable REV7 to suppress CHK1 signaling when ATR activation is unnecessary. Middle: Partial complex activation is achieved through the release of REV7. How REV7 dissociates from the ATR-ATRIP complex is unknown. REV7 is capable of dimerizing, and may detach from the complex upon dimerization and/or interaction with REV7 binding proteins. Top right: Full activation of the ATR complex requires association with its activators. The TOPBP1 binding domain (aa 204-308) in ATRIP includes the REV7 binding sites (P235 and P240). During replication stress, TOPBP1 may replace REV7, fully activating the complex.

and *ATRIP*<sup>P235A, P240A</sup> cells with/without HU. However, the cell cycle profiles of *ATRIP*<sup>P235A, P240A</sup> cells, as well as the BrdU incorporation rates, were similar to WT with/without HU (Supplementary Fig. S8). Therefore, the effects of mutant ATRIP expression on CHK1 phosphorylation are not secondary consequences of an altered cell cycle state. Our results suggest that ablation of REV7–ATRIP binding 1) does not affect the TOPBP1–ATRIP interaction, which is necessary for full activation of ATR, and 2) is independent of p53 accumulation, which is a REV7-dependent pathway.

Next, we investigated the potential role of ATRIP–REV7 interactions in replication stress-induced ATR activation. We hypothesized that dissociation of REV7–ATRIP complexes might facilitate ATR activation in response to DNA replication stress. To test this, 293T cells were transfected with REV7-FH (or empty vector control) and conditionally treated with HU. Then we immunoprecipitated REV7 using FLAG antibodies and measured levels of REV7-associated ATR and ATRIP. Notably, the levels of endogenous ATR and ATRIP in the immunoprecipitated REV7-FH complexes were reduced following HU treatment (Fig. 5B). We conclude that dynamic association and dissociation of REV7 with ATRIP represents a new mechanism for fine-tuning of ATR activation during the DDR.

Finally, we generated a structural model of REV7 in complex with an ATRIP peptide (residues 232–242: VIKPEACSPQF) with excellent convergence using the ColabFold [51] implementation of AlphaFold-Multimer (<https://www.biorxiv.org/content/10.1101/2021.10.04.463034v2>). The structural model was then overlaid with the Cryo-EM structure of the human ATR–ATRIP complex [60] to evaluate whether the complex provides sufficient space for REV7 binding (Figs 5C and D).

Importantly, the ATR–ATRIP complex can phosphorylate CHK1 Ser345 without TOPBP1 [60]. We therefore hypothesized that the Cryo-EM structure of the human ATR–ATRIP complex lacks space for REV7 binding. We found that the REV7 binding peptide resides in a loop region of ATRIP (Fig. 5D). Strikingly, this model suggests that the current Cryo-EM structure of the human ATR–ATRIP complex is spatially incompatible with REV7 binding. However, our immunoprecipitation data, GST-pull down results, and ATR kinase assay results all indicate that REV7 interacts with the ATR–ATRIP complex and affects ATR kinase activity.

Altogether, these data suggest that the local structure of ATRIP may undergo a conformational switch to interact with REV7 and then inhibit ATR kinase activity. We conclude that (1) the REV7–ATRIP–ATR complex is the inactive form, (2) the ATRIP–ATR complex is the partially active form, and (3) the complex of ATRIP–ATR with its activators (TOPBP1, ETAA1, and others) is the fully active form (Fig. 5E).

Taken together, our results suggest that REV7 is an important negative regulator of the ATR–CHK1-mediated S-phase checkpoint. The best-known S-phase function of REV7 involves its association with REV3L to form the TLS extender DNA polymerase, Pol $\zeta$ . Similar to ATR signaling, TLS is initiated by RPA-coated ssDNA. It is generally thought that RPA–ssDNA recruits the RAD18–RAD6 complex to the vicinity of stalled replication forks to promote PCNA monoubiquitylation and switching of replicative DNA polymerases with Y-family inserter TLS polymerases. Depending on the nature of the fork-stalling DNA lesion, inserter polymerases may be switched and replaced with Pol $\zeta$ . Jacobs and colleagues

have shown that REV7 and REV3 reside at stalled and regressed forks and both facilitate ongoing fork movement and promote protection of HU-regressed forks [61]. Many previous studies have demonstrated significant coordination, interplay, and functional redundancy between ATR–CHK1 signaling and TLS. For example, historically, many XPV cell lines (which lack functional Pol $\eta$ ) were found to be sensitive to UV-induced DNA damage only in the presence of caffeine [62, 63], which is now known to inhibit ATR. Kannouche and colleagues formally demonstrated a synthetic lethal relationship (i.e. redundancy) between *POLH* and *ATR* [64]. TLS-compromised cells lacking RAD18 or inserter Y-family DNA polymerases (such as Pol $\kappa$  or Pol $\eta$ ) fail to recover from replication stalling and exhibit persistent compensatory CHK1 signaling. Thus, S-phase checkpoint signaling confers DNA damage tolerance and is induced when TLS fails. Conversely, TLS is important for the timely attenuation of the S-phase checkpoint. In our studies, REV3L-deficiency did not phenocopy the aberrant excessive CHK1 phosphorylation that was induced by REV7-loss. We suggest therefore that REV7 is targeted to ATRIP to attenuate ATR–CHK1 signaling via a mechanism that does not require Pol $\zeta$ . It is remarkable that the small REV7 protein forms specific complexes with multiple partners to regulate TLS, p53 activity, DSB resection, and S-phase checkpoint signaling. Further work is necessary to clarify the mechanisms by which REV7 is directed to its various partners to facilitate and perhaps integrate diverse genome maintenance processes.

Altogether, our results suggest that the TLS pathway may be an important determinant of ATR substrate choice. Further work is needed to clarify the mechanisms by which the TLS pathway directs ATR substrate selection for activation of the cell cycle checkpoint.

## Acknowledgements

We sincerely thank Richard D. Wood (University of Texas MD Anderson Cancer Center) for his early support of this project. We thank Mary Tomida and Luke Tomida for editorial help. Protein identification was provided by the UT Austin Center for Biomedical Research Support Biological Mass Spectrometry Facility (RRID:SCR\_021728).

*Author contributions:* M.B., H.S., and J.T. conceived and designed the experiments. C.V. and J.T. designed the research. M.B., S.K., S.N., S.A., Y.K., S.K., P.Z., C.V., and J.T. performed research. M.B., S.K., S.N., S.A., Y.K., S.K., P.Z., C.V., and J.T. analyzed data. C.V. and J.T. wrote the paper.

## Supplementary data

Supplementary data is available at NAR online.

## Conflict of interest

The authors declare that they have no conflict of interest.

## Funding

This research was supported by National Institutes of Health (NIH) grants 1R15CA263784 and 1R15CA305114 (to J.T.), National Institutes of Health (NIH) grants R01 ES009558, CA215347, and CA229530 (to C.V.); Japan Society for the Promotion of Science (JSPS) KAKENHI Grant 19H04267;

Takeda Bioscience Research grant; Mitsubishi Research grant; Naito Research grant; and Astellas Research Foundation (to H.S.).

## Material availability

This study did not generate unique reagents.

## Data availability

The mass spectrometry proteomics data have been deposited to the ProteomeXchange Consortium via the PRIDE [65] partner repository with the dataset identifier PXD072142. The molecular model of the REV7–ATRIP peptide complex is available in ModelArchive at <https://modelarchive.org/doi/10.5452/ma-v7nod>. All other data are presented in the article.

## Lead contact

Additional information and requests for resources and reagents can be directed to and fulfilled by lead contact, Dr Junya Tomida ([jtomida@charlotte.edu](mailto:jtomida@charlotte.edu)).

## References

- van Gent DC, Hoeijmakers JH, Kanaar R. Chromosomal stability and the DNA double-stranded break connection. *Nat Rev Genet* 2001;2:196–206. <https://doi.org/10.1038/35056049>
- Wood RD, Mitchell M, Lindahl T. Human DNA repair genes. 2005. *Mutat Res* 2005;577:275–83.
- Cimprich KA, Cortez D. ATR: an essential regulator of genome integrity. *Nat Rev Mol Cell Biol* 2008;9:616–27. <https://doi.org/10.1038/nrm2450>
- Matsuura S, Tauchi H, Nakamura A et al. Positional cloning of the gene for Nijmegen breakage syndrome. *Nat Genet* 1998;19:179–81. <https://doi.org/10.1038/549>
- Ogi T, Walker S, Stiff T et al. Identification of the first ATRIP-deficient patient and novel mutations in ATR define a clinical spectrum for ATR–ATRIP seckel syndrome. *PLoS Genet* 2012;8:e1002945. <https://doi.org/10.1371/journal.pgen.1002945>
- Zhang S, Yajima H, Huynh H et al. Congenital bone marrow failure in DNA-PKcs mutant mice associated with deficiencies in DNA repair. *J Cell Biol* 2011;193:295–305. <https://doi.org/10.1083/jcb.201009074>
- Hira A, Yoshida K, Sato K et al. Mutations in the gene encoding the E2 conjugating enzyme UBE2T cause Fanconi anemia. *Am Hum Genet* 2015;96:1001–7. <https://doi.org/10.1016/j.ajhg.2015.04.022>
- Bluteau D, Masliah-Planchon J, Clairmont C et al. Biallelic inactivation of REV7 is associated with Fanconi anemia. *J Clin Invest* 2016;126:3580–4. <https://doi.org/10.1172/JCI88010>
- Xu X, Xu Y, Guo R et al. Fanconi anemia proteins participate in a break-induced-replication-like pathway to counter replication stress. *Nat Struct Mol Biol* 2021;28:487–500. <https://doi.org/10.1038/s41594-021-00602-9>
- O'Neill T, Dwyer AJ, Ziv Y et al. Utilization of oriented peptide libraries to identify substrate motifs selected by ATM. *J Biol Chem* 2000;275:22719–27. <https://doi.org/10.1074/jbc.M001002200>
- Lempiainen H, Halazonetis TD. Emerging common themes in regulation of PIKKs and PI3Ks. *EMBO J* 2009;28:3067–73. <https://doi.org/10.1038/emboj.2009.281>
- Lovejoy CA, Cortez D. Common mechanisms of PIKK regulation. *DNA Repair (Amst)* 2009;8:1004–8. <https://doi.org/10.1016/j.dnarep.2009.04.006>
- Blackford AN, Jackson SP. ATM, ATR, and DNA-PK: the trinity at the Heart of the DNA damage response. *Mol Cell* 2017;66:801–17. <https://doi.org/10.1016/j.molcel.2017.05.015>
- Brown EJ, Baltimore D. ATR disruption leads to chromosomal fragmentation and early embryonic lethality. *Genes Dev* 2000;14:397–402. <https://doi.org/10.1101/gad.14.4.397>
- Zou L, Elledge SJ. Sensing DNA damage through ATRIP recognition of RPA–ssDNA complexes. *Science* 2003;300:1542–8. <https://doi.org/10.1126/science.1083430>
- Fanning E, Klimovich V, Nager AR. A dynamic model for replication protein A (RPA) function in DNA processing pathways. *Nucleic Acids Res* 2006;34:4126–37. <https://doi.org/10.1093/nar/gkl550>
- Yan S, Michael WM. TopBP1 and DNA polymerase-alpha directly recruit the 9-1-1 complex to stalled DNA replication forks. *J Cell Biol* 2009;184:793–804. <https://doi.org/10.1083/jcb.200810185>
- Ohashi E, Takeishi Y, Ueda S et al. Interaction between Rad9–Hus1–Rad1 and TopBP1 activates ATR–ATRIP and promotes TopBP1 recruitment to sites of UV-damage. *DNA Repair (Amst)* 2014;21:1–11. <https://doi.org/10.1016/j.dnarep.2014.05.001>
- Feng S, Zhao Y, Xu Y et al. Ewing tumor-associated antigen 1 interacts with replication protein A to promote restart of stalled replication forks. *J Biol Chem* 2016;291:21956–62. <https://doi.org/10.1074/jbc.C116.747758>
- Haahr P, Hoffmann S, Tollenaere MA et al. Activation of the ATR kinase by the RPA-binding protein ETAA1. *Nat Cell Biol* 2016;18:1196–207. <https://doi.org/10.1038/ncb3422>
- Kobayashi M, Hayashi N, Takata M et al. NBS1 directly activates ATR independently of MRE11 and TOPBP1. *Genes Cells* 2013;18:238–46. <https://doi.org/10.1111/gtc.12031>
- Matsuoka S, Ballif BA, Smogorzewska A et al. ATM and ATR substrate analysis reveals extensive protein networks responsive to DNA damage. *Science* 2007;316:1160–6. <https://doi.org/10.1126/science.1140321>
- Lukas J, Lukas C, Bartek J. Mammalian cell cycle checkpoints: signalling pathways and their organization in space and time. *DNA Repair (Amst)* 2004;3:997–1007. <https://doi.org/10.1016/j.dnarep.2004.03.006>
- Lane DP. Cancer. p53, guardian of the genome. *Nature* 1992;358:15–6. <https://doi.org/10.1038/358015a0>
- Helton ES, Chen X. p53 modulation of the DNA damage response. *J Cell Biochem* 2007;100:883–96. <https://doi.org/10.1002/jcb.21091>
- Zhao H, Piwnicka-Worms H. ATR-mediated checkpoint pathways regulate phosphorylation and activation of human Chk1. *Mol Cell Biol* 2001;21:4129–39. <https://doi.org/10.1128/MCB.21.13.4129-4139.2001>
- Tibbetts RS, Brumbaugh KM, Williams JM et al. A role for ATR in the DNA damage-induced phosphorylation of p53. *Genes Dev* 1999;13:152–7. <https://doi.org/10.1101/gad.13.2.152>
- Li Z, Wang-Heaton H, Cartwright BM et al. ATR prevents Ca(2+) overload-induced necrotic cell death through phosphorylation-mediated inactivation of PARP1 without DNA damage signaling. *FASEB J* 2021;35:e21373. <https://doi.org/10.1096/fj.202001636RRR>
- Kratz K, de Lange T. Protection of telomeres 1 proteins POT1a and POT1b can repress ATR signaling by RPA exclusion, but binding to CST limits ATR repression by POT1b. *J Biol Chem* 2018;293:14384–92. <https://doi.org/10.1074/jbc.RA118.004598>
- Sasanuma H, Tsuda M, Morimoto S et al. BRCA1 ensures genome integrity by eliminating estrogen-induced pathological topoisomerase II–DNA complexes. *Proc Natl Acad Sci USA* 2018;115:E10642–51. <https://doi.org/10.1073/pnas.1803177115>
- Saha LK, Kim S, Kang H et al. Differential micronucleus frequency in isogenic human cells deficient in DNA repair pathways is a valuable indicator for evaluating genotoxic agents and their genotoxic mechanisms. *Environ and Mol Mutagen* 2018;59:529–38. <https://doi.org/10.1002/em.22201>

32. Aricescu AR, Lu W, Jones EY. A time- and cost-efficient system for high-level protein production in mammalian cells. *Acta Crystallogr D Biol Crystallogr* 2006;62:1243–50. <https://doi.org/10.1107/S0907444906029799>
33. Lee YS, Gregory MT, Yang W. Human Pol zeta purified with accessory subunits is active in translesion DNA synthesis and complements Pol eta in cisplatin bypass. *Proc Natl Acad Sci USA* 2014;111:2954–9. <https://doi.org/10.1073/pnas.1324001111>
34. Biller M, Kabir S, Boado C *et al*. REV7-p53 interaction inhibits ATM-mediated DNA damage signaling. *Cell Cycle* 2024;23:339–52. <https://doi.org/10.1080/15384101.2024.2333227>
35. Kratz K, Artola-Boran M, Kobayashi-Era S *et al*. FANCD2-associated nuclease 1 partially compensates for the lack of exonuclease 1 in mismatch repair. *Mol Cell Biol* 2021;41:e0030321. <https://doi.org/10.1128/MCB.00303-21>
36. Tsuda M, Terada K, Ooka M *et al*. The dominant role of proofreading exonuclease activity of replicative polymerase epsilon in cellular tolerance to cytarabine (Ara-C). *Oncotarget* 2017;8:33457–74. <https://doi.org/10.18632/oncotarget.16508>
37. Ibrahim MA, Yasui M, Saha LK *et al*. Enhancing the sensitivity of the thymidine kinase assay by using DNA repair-deficient human TK6 cells. *Environ and Mol Mutagen* 2020;61:602–10. <https://doi.org/10.1002/em.22371>
38. Takeuchi R, Oshige M, Uchida M *et al*. Purification of Drosophila DNA polymerase zeta by REV1 protein-affinity chromatography. *Biochem J* 2004;382:535–43. <https://doi.org/10.1042/BJ20031833>
39. Takata K, Shimizu T, Iwai S *et al*. Human DNA polymerase N (POLN) is a low fidelity enzyme capable of error-free bypass of 5S-thymine glycol. *J Biol Chem* 2006;281:23445–55. <https://doi.org/10.1074/jbc.M604317200>
40. Tomida J, Takata K, Lange SS *et al*. REV7 is essential for DNA damage tolerance via two REV3L binding sites in mammalian DNA polymerase zeta. *Nucleic Acids Res* 2015;43:1000–11. <https://doi.org/10.1093/nar/gku1385>
41. Tomida J, Itaya A, Shigechi T *et al*. A novel interplay between the Fanconi anemia core complex and ATR–ATRIP kinase during DNA cross-link repair. *Nucleic Acids Res* 2013;41:6930–41. <https://doi.org/10.1093/nar/gkt467>
42. Takata K, Reh S, Tomida J *et al*. Human DNA helicase HELQ participates in DNA interstrand crosslink tolerance with ATR and RAD51 paralogs. *Nat Commun* 2013;4:2338. <https://doi.org/10.1038/ncomms3338>
43. Tomida J, Takata KI, Bhetawal S *et al*. FAM35A associates with REV7 and modulates DNA damage responses of normal and BRCA1-defective cells. *EMBO J* 2018;37:e99543. <https://doi.org/10.15252/embj.201899543>
44. Yousefzadeh MJ, Wyatt DW, Takata K *et al*. Mechanism of suppression of chromosomal instability by DNA polymerase POLQ. *PLoS Genet* 2014;10:e1004654. <https://doi.org/10.1371/journal.pgen.1004654>
45. Martin SK, Tomida J, Wood RD. Disruption of DNA polymerase zeta engages an innate immune response. *Cell Rep* 2021;34:108775. <https://doi.org/10.1016/j.celrep.2021.108775>
46. Sarbassov DD, Guertin DA, Ali SM *et al*. Phosphorylation and regulation of Akt/PKB by the rictor-mTOR complex. *Science* 2005;307:1098–101. <https://doi.org/10.1126/science.1106148>
47. Barr SM, Leung CG, Chang EE *et al*. ATR kinase activity regulates the intranuclear translocation of ATR and RPA following ionizing radiation. *Curr Biol* 2003;13:1047–51. [https://doi.org/10.1016/S0960-9822\(03\)00376-2](https://doi.org/10.1016/S0960-9822(03)00376-2)
48. Vaziri C, Saxena S, Jeon Y *et al*. A p53-dependent checkpoint pathway prevents rereplication. *Mol Cell* 2003;11:997–1008. [https://doi.org/10.1016/S1097-2765\(03\)00099-6](https://doi.org/10.1016/S1097-2765(03)00099-6)
49. Gao Y, Mutter-Rottmayer E, Greenwalt AM *et al*. A neomorphic cancer cell-specific role of MAGE-A4 in trans-lesion synthesis. *Nat Commun* 2016;7:12105. <https://doi.org/10.1038/ncomms12105>
50. Yang Y, Gao Y, Mutter-Rottmayer L *et al*. DNA repair factor RAD18 and DNA polymerase Polkappa confer tolerance of oncogenic DNA replication stress. *J Cell Biol* 2017;216:3097–115. <https://doi.org/10.1083/jcb.201702006>
51. Mirdita M, Schutze K, Moriwaki Y *et al*. ColabFold: making protein folding accessible to all. *Nat Methods* 2022;19:679–82. <https://doi.org/10.1038/s41592-022-01488-1>
52. Tunyasuvunakool K, Adler J, Wu Z *et al*. Highly accurate protein structure prediction for the human proteome. *Nature* 2021;596:590–6. <https://doi.org/10.1038/s41586-021-03828-1>
53. de Krijger I, Boersma V, Jacobs JLL. REV7: jack of many trades. *Trends Cell Biol* 2021;31:686–701. <https://doi.org/10.1016/j.tcb.2021.04.002>
54. Mordes DA, Glick GG, Zhao R *et al*. TopBP1 activates ATR through ATRIP and a PIKK regulatory domain. *Genes Dev* 2008;22:1478–89. <https://doi.org/10.1101/gad.1666208>
55. Wang J, Han X, Zhang Y. Autoregulatory mechanisms of phosphorylation of checkpoint kinase 1. *Cancer Res* 2012;72:3786–94. <https://doi.org/10.1158/0008-5472.CAN-12-0523>
56. Niida H, Katsuno Y, Banerjee B *et al*. Specific role of Chk1 phosphorylations in cell survival and checkpoint activation. *Mol Cell Biol* 2007;27:2572–81. <https://doi.org/10.1128/MCB.01611-06>
57. Gatei M, Sloper K, Sorensen C *et al*. Ataxia-telangiectasia-mutated (ATM) and NBS1-dependent phosphorylation of Chk1 on Ser-317 in response to ionizing radiation. *J Biol Chem* 2003;278:14806–11. <https://doi.org/10.1074/jbc.M210862200>
58. Bi X, Slater DM, Ohmori H *et al*. DNA polymerase kappa is specifically required for recovery from the benzo[a]pyrene-dihydrodiol epoxide (BPDE)-induced S-phase checkpoint. *J Biol Chem* 2005;280:22343–55. <https://doi.org/10.1074/jbc.M501562200>
59. Bi X, Barkley LR, Slater DM *et al*. Rad18 regulates DNA polymerase kappa and is required for recovery from S-phase checkpoint-mediated arrest. *Mol Cell Biol* 2006;26:3527–40. <https://doi.org/10.1128/MCB.26.9.3527-3540.2006>
60. Rao Q, Liu M, Tian Y *et al*. Cryo-EM structure of human ATR–ATRIP complex. *Cell Res* 2018;28:143–56. <https://doi.org/10.1038/cr.2017.158>
61. Paniagua I, Tayeh Z, Falcone M *et al*. MAD2L2 promotes replication fork protection and recovery in a shieldin-independent and REV3L-dependent manner. *Nat Commun* 2022;13:5167. <https://doi.org/10.1038/s41467-022-32861-5>
62. Kannouche P, Broughton BC, Volker M *et al*. Domain structure, localization, and function of DNA polymerase eta, defective in xeroderma pigmentosum variant cells. *Genes Dev* 2001;15:158–72. <https://doi.org/10.1101/gad.187501>
63. Itoh T, Linn S, Kamide R *et al*. Xeroderma pigmentosum variant heterozygotes show reduced levels of recovery of replicative DNA synthesis in the presence of caffeine after ultraviolet irradiation. *J Invest Dermatol* 2000;115:981–5. <https://doi.org/10.1046/j.1523-1747.2000.00154.x>
64. Despras E, Daboussi F, Hyrien O *et al*. ATR/Chk1 pathway is essential for resumption of DNA synthesis and cell survival in UV-irradiated XP variant cells. *Hum Mol Genet* 2010;19:1690–701. <https://doi.org/10.1093/hmg/ddq046>
65. Perez-Riverol Y, Bandla C, Kundu DJ *et al*. The PRIDE database at 20 years: 2025 update. *Nucleic Acids Res* 2025;53:D543–53. <https://doi.org/10.1093/nar/gkae1011>